



# HHS Public Access

Author manuscript

Nat Chem Biol. Author manuscript; available in PMC 2010 June 01.

Published in final edited form as:

Nat Chem Biol. 2009 December ; 5(12): 929–935. doi:10.1038/nchembio.244.

## Spatiotemporal modulation of biodiversity in a synthetic chemical-mediated ecosystem

Hao Song, Stephen Payne, Meagan Gray, and Lingchong You\*

Department of Biomedical Engineering and Institute for Genome Sciences and Policy, Duke University, Durham, NC 27708 USA

### Abstract

Biodiversity, or the relative abundance of species, measures the persistence of an ecosystem. To better understand its modulation, we analyzed the spatial and temporal dynamics of a synthetic, chemical-mediated ecosystem that consisted of two engineered *Escherichia coli* populations. Depending on the specific experimental conditions implemented, the dominant interaction between the two populations could be competition for nutrients or predation due to engineered communication. While the two types of interactions resulted in different spatial patterns, they demonstrated a common trend in terms of the modulation of biodiversity. Specifically, biodiversity decreased with increasing cellular motility if the segregation distance between the two populations was comparable to the length scale of the chemical-mediated interaction. Otherwise, biodiversity was insensitive to cellular motility. Our results suggested a simple criterion for predicting the modulation of biodiversity by habitat partitioning and cellular motility in chemical-mediated ecosystems.

---

Microbial ecosystems play fundamental roles in a wide variety of biological processes, including biogeochemical cycles in the biosphere 1–3, immunological defense against pathogens by gut microbiota 4,5, and engineered microbial consortia for biotechnological applications<sup>6</sup>. One important characteristic of microbial ecosystems is biodiversity, which represents species richness and relative abundance in relation to one another<sup>7</sup>. A central challenge in microbial ecology is to elucidate the mechanisms underlying the maintenance of biodiversity, a vital element in determining the persistence and functionality of ecological communities 8–16.

There are two types of cell-to-cell interactions in microbial ecosystems<sup>17,18</sup>. The first type occurs locally or requires direct cell-cell contact. One microbial species, for example, may kill another by contact. This contact may occur by epibiotic means (e.g., *Vampirococcus* attaches to the outer surface of *Chromatium* to induce killing<sup>19,20</sup>), by periplasmic

---

Users may view, print, copy, download and text and data- mine the content in such documents, for the purposes of academic research, subject always to the full Conditions of use: [http://www.nature.com/authors/editorial\\_policies/license.html#terms](http://www.nature.com/authors/editorial_policies/license.html#terms)

\*To whom correspondence should be addressed. you@duke.edu Phone: (919)660-8408. Fax: (919)668-0795. Mailing Address: CIEMAS 2345, 101 Science Drive, Box 3382, Durham, NC 27708 USA.

**Author Contributions** H.S. and L.Y. conceived the project; H.S., S.P. and M.G. performed the experiments; H.S. performed the mathematical modeling; H.S., S.P. and L.Y. analyzed the data; H.S., S.P., and L.Y. wrote the paper.

### Competing financial interests

The authors declare that they have no conflict of interest.

invasion (e.g. *Bdellovibrio* upon gram-negative prokaryotes 21), or by invasion into the cytoplasm (e.g., *Daptobacter* upon *Chromatium minus* 19).

The second type occurs *via* small diffusible chemicals. This can happen when microbes compete for shared, diffusible nutrients or chemoattractants, when each species excretes an essential metabolite for the survival of the other, forming a mutualistic relationship 22, or when predator cells excrete diffusible hydrolytic enzymes that degrade and digest prey cells to generate diffusible nutrient molecules, which contribute to the predator's survival (e.g., both *Myxococcus* and *Lysobacter* use lytic enzymes to prey upon other bacteria 23–25). Such chemical-mediated interactions play essential roles in determining many behavioral responses of microbes, such as sex, alarm and aggregation as well as predation 26–34.

Studies have highlighted the importance of cellular motility in determining biodiversity in model ecosystems with local interactions: reducing motility or dispersal promotes biodiversity 35,36. However, it remains vague how motility can impact biodiversity in chemical-mediated ecosystems where interactions can happen at longer length scales. Specifically, how does the combination of cellular motility and long-range interactions *via* diffusible chemicals affect biodiversity?

To address this question, we employed a synthetic chemical-mediated predator-prey ecosystem 37 (see Fig. S1 and Methods). This system consists of two engineered *E. coli* populations mediated by quorum-sensing (QS). The predator kills the prey by inducing expression of a killer protein (CcdB), whereas the prey rescues the predator by inducing expression of an antidote (CcdA) in the predator. The two populations also compete for shared resources in co-culture (Fig. 1a). Thereby, the programmed predation and the competition for nutrients occur through chemical diffusion. Overall, this synthetic system resembles many natural chemical-mediated predator-prey ecosystems in terms of their interaction characteristics, both of which involve diffusion-mediated interactions. We note that such ecological interactions have also been implemented using different strategies. In particular, several interesting synthetic ecosystems based on airborne inter- and intra-kingdom communication, including commensalism, mutualism, parasitism and predator-prey ecosystems were constructed recently 38. In their synthetic predator-prey ecosystem, the predator (*E. coli*) inhibited the prey (mammalian CHO cell) by outgrowing the prey; meanwhile, the prey synthesized and secreted  $\beta$ -lactamase (sBLA) which hydrolyzed ampicillin in the culture to promote survival of the predator 38. Such a synthetic predator-prey ecosystem also involves two modes of chemical-mediated interactions, competition and predator-prey.

We found that, in our synthetic ecosystem, cellular motility had a negligible impact on biodiversity when the predator and prey cells were well-mixed in either liquid phase or soft agar. In contrast, decreasing motility promoted biodiversity when the predator and the prey were inoculated at a sufficient segregation distance on soft agar. The seemingly discrepant role of motility on biodiversity could be attributed to the existence of two critical segregation distances between the predator and the prey, as revealed by a mathematical model that described the spatiotemporal dynamics of the system. These results led us to the following conclusion: in a two-population chemical-mediated ecosystem, the biodiversity

was significantly modulated by motility if the segregation distance between the two populations was comparable to the interaction distance defined by the communication signals. Our results also indicated that the spatial distribution patterns of populations may result from different dominating modes of interactions. For example, in predation, the cell distribution pattern revealed a growth preference of the predator in the vicinity of the prey; however, in competition, the competitor grew in a largely uniform manner and was insensitive to the distance from the other competitor.

## Results

### Responses of predator and prey to growth and killing signals

We first characterized basic growth dynamics of the predator and the prey cells in both solid and liquid phases (see Supplementary Methods) in response to the growth and killing signals (Figs. 1b–d and Supplementary Results, Fig. S2). In each solid-phase experiment, growth was initiated from a 10 $\mu$ l overnight culture and measured by fluorescence imaging. Consistent with the system design logic (Fig. S1), growth and expansion of the predator was significantly inhibited by Isopropyl  $\beta$ -D-1-thiogalactopyranoside (IPTG **1**) but further restored by 3-oxohexanoyl-homoserine lactone (3OC6HSL **2**) (Figs. 1b, c). In contrast, growth and expansion of the prey was only inhibited when both IPTG and 3-oxododecanoyl-homoserine lactone (3OC12HSL **3**) were present (Figs. 1b, d). Similar results were obtained in the liquid phase (Fig. S2). Furthermore, our results confirmed the predation interaction between the predator and the prey: the predator expansion was enhanced by the prey whereas the prey expansion was drastically inhibited by the predator (Figs. 1c, d red lines; Fig 1b right panel).

We noted that MG1655 cells containing the prey construct grew better upon IPTG induction (Fig. 1d and Fig. S2B). A similar observation was made in the literature 39, and it was proposed that IPTG might promote growth of wild-type *E. coli* by influencing its global metabolism. This phenomenon might have partially masked the effects of programmed killing by IPTG-induced CcdBs; thus, the killing of the MG1655 predator was not complete (~50% reduction of cell density in solid phase, Fig. 1c). In Top10F<sup>+</sup> cells, where the “hidden benefit” of IPTG induction was insignificant, IPTG-induced predator killing was much more drastic (Fig. S3A).

### Motility had a negligible impact on biodiversity with well-mixed predator and prey

To quantify biodiversity in a mixed culture, we used the modified Simpson’s biodiversity index (BI) 7:  $BI=1 - \sum_{i=1}^2 x_i^2=2x_1x_2$ , where  $x_i$  is the fraction of the  $i$ th population in a co-culture ( $i=1$  for the predator and 2 for the prey). In a liquid culture,  $x_i$  was calculated by using the densities of the two populations (e.g.,  $x_1$  = predator density/total density). In a solid culture,  $x_i$  was calculated by using the average densities over a spatial domain ( $\Omega$ ).

$$x_i = \frac{\int_{\Omega} p_i dx dy}{\int_{\Omega} p_1 dx dy + \int_{\Omega} p_2 dx dy} \quad (1)$$

where  $p_i$  is the density distribution in  $\Omega$  for population  $i$ . In either case, the BI reached a maximum for  $x_1 = x_2 = 0.5$  (Fig. 2a).

To guide our experiments, we modeled system dynamics using partial differential equations (PDE, see Supplementary Methods and Eqs. S1–S5) for the solid phase and ordinary differential equations (ODE, Eqs. S8–S12) for the liquid phase. The ODE model accounted for cell growth and interactions (*via* QS-induced killing and rescuing), gene expression, and QS signals synthesis and degradation. The PDE model further accounted for spatial factors such as cellular motion by diffusion and chemotaxis 40–43 and signal diffusion (see Supplementary Methods for details).

We first examined the effects of motility on biodiversity of well-mixed cultures in two extreme cases: the liquid environment allowing maximum cellular motility and the solid environment with drastically reduced motility. We simulated the solid-phase dynamics by initial random arrangement of the predator and the prey cells over the spatial domain with a uniform distribution. Simulation indicated that the spatial average densities of the two populations in the solid phase (Fig. 2b inset, dots) were similar to those in the liquid phase (Fig. 2b inset, lines). As a result, the BI was similar for both conditions (Fig. 2b), indicating negligible effects of motility. In addition, modeling showed that the BI would decrease with time due to programmed predation, leading an initial, approximately equal amount of predator and prey (BI $\approx$ 0.5) to the state in which the predator significantly exceeded the prey (BI $\approx$ 0.1). To experimentally test these predictions, we used fluorescence microscopy to measure biodiversity in both a liquid culture and a solid culture at 5hr, 12hr, and 24hr post inoculation. These time points corresponded to the states before and after a culture reached its stationary state when nutrients were largely exhausted (see Supplementary Methods). This short incubation time also helped prevent mutants that might escape circuit control from dominating the culture. We noted that these quantifications focused on the temporal dynamics, not the asymptotic steady-state of the system, since recent studies emphasized the importance of the transient dynamics rather than the long-term behavior of ecological systems 44. Examination of transient ecological dynamics could provide a more relevant understanding of how population levels would change over time. Consistent with the model prediction, our experimental results showed that the BI decreased with time until settling at  $\sim$ 0.1 after 12 hrs (Fig. 2c). They also showed that the biodiversity in the solid phase was essentially identical to that in the liquid phase (Fig. 2c), also consistent with the model prediction.

This observation was counterintuitive in the context of previous work that underscored the significant influence of motility on biodiversity 36. To gain further insight, we simulated the spatial distributions of the predator for varying motility (Fig. S4A). We found that, with zero motility ( $D_{cell} = 0$ ), the coefficient of variation (CV = standard deviation/mean) of the predator distribution did not change significantly with time (Fig. S4B, same for the prey (not shown)). When cells were slightly motile ( $D_{cell} = 10^{-4}$  cm<sup>2</sup>/hr), the CV gradually decreased over time. At a sufficiently high motility ( $D_{cell} = 5 \times 10^{-3}$  cm<sup>2</sup>/hr), the CV vanished quickly. Although motility significantly affected the variance of the populations' spatial density distribution, it did not affect the ratio of their spatially averaged densities ( $\langle$ predator $\rangle$ /

<prey>) or the BI over the entire spatial domain (Fig. S4C). These results again indicated that motility appeared to have a negligible influence on the biodiversity of this ecosystem.

### Reduced motility could promote biodiversity in partitioned habitats

Studies on the metapopulation dynamics in ecosystems suggested that habitat partitioning might affect biodiversity<sup>45–49</sup>. We thus sought to examine how habitat configuration, in conjunction with motility, could affect biodiversity in our system. To simulate habitat partitioning, we seeded the predator and the prey separately at two focal points with varying distance in between, leaving the other locations with zero density. Our model predicted that increasing the segregation distance between the seeding points would promote biodiversity (Fig. 3a). If the predator and prey were seeded together ( $d = 0$ ), the predator would disperse outward at a faster speed than the prey due to its growth advantage gained from the prey's rescue. The outward dispersion of the predator would deplete chemoattractants in its path (Fig. S5), which would trap the prey at the inoculation point. Increasing the segregation distance between the two populations (e.g.,  $d = 1$  and  $2$  cm) would reduce the strength of long-range interactions, including killing and rescuing by the diffusible AHL signals and competition for chemoattractants and nutrients. This reduction would lead to less killing, faster growth, and more chemotaxis of the prey, resulting in a larger prey territory and density. To test the prediction experimentally, we seeded 10 $\mu$ l predator cells and 10 $\mu$ l prey cells at two separate locations with increasing distances ( $d = 0, 1, \text{ or } 2$  cm) on pH-buffered soft (0.2%) M9 agar plates, which were incubated at 37°C for 20 hrs. We then measured the cell densities by fluorescence imaging (see details in Supplementary Methods). Figure 3b showed that the biodiversity indeed increased with increasing segregation distance, consistent with the model prediction (Fig. 3a). In particular, increasing initial partitioning distance from 0cm to 2cm increased the BI from  $\sim 0.07$  to  $\sim 0.37$  (0.3% agar).

Our model further predicted that decreasing motility would increase biodiversity when the populations were sufficiently segregated (Fig. 3a,  $d = 1$  cm or  $2$  cm). This was mainly because motility affected the spatiotemporal interaction strengths between the predator and the prey under this condition. At a higher motility, the predator and the prey would approach each other at a faster speed; in turn, the prey would experience a higher level of 3OC12HSL secreted and diffused from the predator, thereby exhibiting a stronger predation effect. However, at a lower motility, the two populations would approach each other slowly; in turn, the prey would experience less killing, leading to faster prey growth and higher biodiversity. Again, this prediction was validated by experiments: at  $d = 1$  cm or  $2$  cm, decreasing motility by reducing the agar density from 0.2% to 0.3% increased the BI by about 2~3 fold (Fig. 3b).

We further noticed that the promotion of biodiversity by motility with sufficient habitat partitioning did not require induced predation. For instance, without IPTG induction, the dominant interaction in our system was competition for nutrients (Fig. 1a). For the pair implemented in MG1655 cells, the uninduced predator had a significant growth advantage over the uninduced prey (Fig. 1b). Our results revealed two salient points. First, the spatial patterns and the biodiversity indices resulting from competition (see Supplementary Results, Fig. S6) were significantly different from those due to induced predation (Fig. 3), as

highlighted by the detailed comparison of the predator's spatial patterns (Fig. S7). Second, similar to the case with induced predation (Fig. 3), reduced motility also increased biodiversity when the two populations were sufficiently segregated (Fig. S6,  $d = 1\text{cm}$  or  $2\text{cm}$ ). Furthermore, the latter conclusion did not depend on chemotaxis either. In Top10F' cells, which can diffuse in thin agar but with impaired chemotax, reduced motility also promoted biodiversity with sufficient segregation distance, as revealed by both modeling and experiments (Figs. S3B, D, F). However, this motility-mediated biodiversity modulation became negligible when competing populations had similar growth rates: neither motility nor segregation distance impacted biodiversity (see Supplementary Results, Figs. S3C, E, G (Top10F') and Fig. S8 (MG1655)).

These analyses also revealed a potential limitation of the biodiversity index. As a lumped metric, it is convenient to use for summarizing system dynamics and has revealed a commonality between predation and competition in terms of the contributions of motility and population segregation to biodiversity. However, the metric can mask important differences in the spatiotemporal patterns resulting from different interactions. When predation was induced by IPTG, cell distribution patterns revealed a growth preference of the predator in the vicinity of the prey (Fig. S7A). Without IPTG induction, the uninduced predator population expanded almost uniformly from the seeding point toward all directions except near the uninduced prey population (Fig. S7B). This difference in pattern formation was also qualitatively captured by our model (Figs. S7C, D). However, since our model is drastically simplified (see Supplementary Methods and Reference 37), some fine details of the experimental patterns were not quantitatively captured by our model. Together, a combination of biodiversity index and population distribution patterns would provide a comprehensive picture of the commonality and difference in the system dynamics, with or without induced predation.

### Effects of motility as constrained by two critical segregation distances

Our results appeared to suggest a conflicting role of motility in modulating biodiversity. When the predator and the prey were seeded in close proximity, motility had a negligible impact on biodiversity; when they were seeded separately, motility had a drastic impact on biodiversity. To resolve this apparent paradox, we examined the interplay between segregation distance and motility by simulation. We initiated each simulation by seeding individual cells in random patches separated by barren zones containing no cells (Fig. S9A). Also, the predator and the prey were not seeded in the same patch. By modifying the area of the barren zones, we could modulate the average segregation distance between the two populations. A typical result was shown in Fig. S9B, where we examined the dependence of biodiversity on the segregation distance at a fixed cellular motility ( $D_{cell} = 10^{-3} \text{ cm}^2/\text{hr}$ ). It showed that an increasing segregation distance ( $d$ ) had little impact on biodiversity until  $d$  exceeded a critical value ( $d_{c1}$ ), where the dependence of the BI on  $d$  went through a distinct transition. When  $d > d_{c1}$ , the BI increased almost proportionally with an increasing  $d$  until  $d$  reached another critical distance  $d_{c2}$ . When  $d > d_{c2}$ , the BI again was independent of the furthering increment of  $d$  (Fig. S9B).

The same trend relating segregation distance to biodiversity could be captured by 1-D simulations, which were much more efficient computationally. We initiated each simulation by seeding the predator and the prey at two focal points with a distance  $d$ , while setting the other places empty (Fig. 4a). Similar to the 2D simulations (Fig. S9), we could then determine the BI from the resulting predator and prey distributions (Fig. 4a). Under the same conditions, similar to the 2D results (Fig. S9B), 1D simulations also identified two critical transition points ( $d_{c1}$  and  $d_{c2}$ ) in the dependence of the BI on  $d$  (Fig. 4b). After the system reached stationary phase upon nutrient depletion, the dependence of the BI on  $d$  was approximately invariant with time (data not shown).

These transitions could be attributed to varying coupling strength by the diffusible nutrients and QS signals. When  $d < d_{c1}$ , the chemical-mediated interactions were dominant, sufficiently strong, and did not depend significantly on small variations of the cells' positions. Therefore, cell motility would not influence the strength of cell-cell communication and the biodiversity in this ecosystem (Fig. 4c, red line). When  $d_{c1} < d < d_{c2}$ , however, the concentrations of chemicals (AHLs and nutrients) experienced by cells varied significantly with their positions, which in turn could be affected by their motility. This effect led to a drastically reduced biodiversity with increasing cellular motility (Fig. 4c, blue line). When  $d > d_{c2}$ , the interaction between the populations was extremely weak and cellular movement would have a negligible contribution to the interaction and biodiversity (Fig. 4c, green line). When induced, the dominant interaction in our system was programmed predation by QS. We thus examined how the critical segregation distances ( $d_{c1}$ ,  $d_{c2}$ ) would change with diffusivity of the QS signals ( $D_{AHL}$ ), and found that both  $d_{c1}$  and  $d_{c2}$  increased with the length scale of the chemical diffusion ( $d_L$ ) (Fig. 4d). The dependence curves divided the phase diagram in the " $d_c-d_L$ "-parameter plane into three regions. In the upper and lower regions, motility had a negligible influence on biodiversity; in contrast, in the middle region, motility drastically influenced biodiversity (Fig. 4d).

## Discussion

While chemical communication is widespread and central to many microbial ecosystems, it has been largely neglected in studies on the maintenance of biodiversity. It has been suggested that decreasing motility increases biodiversity in an ecosystem with local interactions<sup>35,36</sup>. However, our results suggested a more complex picture in a chemical-mediated system, where the biodiversity critically depended on the interplay between cellular motility (by diffusion and chemotaxis), chemical diffusion (of QS signaling chemicals and nutrients), and habitat configuration. We further developed a highly simplified, conceptual model to delineate how motility impacts cellular response at different segregation distances (see Fig. 5a and its legend). The " $R-d$ " dependence revealed two critical segregation distances,  $d_{c1}$  and  $d_{c2}$  (logically similar to Fig. 4b). When  $d < d_{c1}$  or  $d > d_{c2}$ , motility had a negligible influence on the response. When  $d_{c1} < d < d_{c2}$ , however, motility drastically influenced the response.

In summary, motility's impact on biodiversity was determined by the relative magnitudes of the interaction length scale and the segregation distance between populations, as schematized in Fig. 5b. If the interaction length scale was much longer or much shorter than

the segregation distance, motility had little impact on biodiversity. Otherwise, motility would significantly impact biodiversity. In our system, the interactions were mediated by chemical diffusion, which had a longer length scale than motility. The populations thus needed to be segregated sufficiently, but not too far, to manifest the effects of motility (Fig. 4c). In contact-based ecosystems, however, interactions occurred by physical contact and their length scale was that of cellular motility, which was comparable to the segregation distance between cells. In this scenario, motility had a significant impact on biodiversity, which provided an intuitive understanding of past studies on systems with local interactions 35,36. Our conclusion held for other chemical-based interactions between two populations, including competition (Fig. S6). It would be interesting to explore if this conclusion would also hold for ecosystems with many populations in further studies. If so, Fig. 5b would represent a general, qualitative criterion that outlined the contribution of the three factors to biodiversity in a wide variety of ecosystems and that allowed for the classification of ecosystems based on the length scale of their interactions.

Efforts in engineering gene circuits have focused on pushing the limit in the ability to create systems with increasing complexity. The design of synthetic ecosystems represents a new frontier<sup>6</sup> and involves programming different types of cell-cell interactions, such as mutualism 22,38,49, consensus 50, and predation 37,38. Consisting of well-characterized parts, these systems offer unprecedented flexibility to manipulate and analyze interactions between populations, as has been done in this work. The knowledge gained from such investigations may provide novel insights into naturally occurring ecosystem interactions. However, most studies in synthetic ecology have been confined to mimicking basic ecological interactions. Our study represents a significant advance in exploring ecological questions with a synthetic ecosystem.

## Methods

### General methods

See Supplementary Methods for the detailed experimental protocols and the development of the mathematical model and simulations. For the mathematical model (Eqs. S1–S5), the basal parameter values were estimated from literature or fitted to our experimental data (See Supplementary Table S1 and Figs. S10–S12).

### Design logic of the synthetic ecosystem

Our synthetic ecosystem consisted of two *E. coli* populations that regulate each other's gene expression and survival by engineered communication. The predator contained *luxR/lasI* quorum sensing (QS) genes, a *ccdA* antidote gene, and a *ccdB* killer gene (Fig. S1). The prey contained *luxI/lasR* QS genes and *ccdB*. Furthermore, the predator expressed GFPuv(Iva) and the prey expressed mCherry, which allowed us to quantify the two populations by fluorescence. The plasmids carried by the predator and the prey were verified by sequencing.

The two circuits were both under the control of IPTG. Without IPTG induction, the two populations only competed for nutrients in a co-culture. With IPTG induction, the predator

growth would be inhibited by CcdB. CcdB killer protein, a toxin targeting the essential gyrase of *E. coli*, inhibited cell growth and caused cell death. The CcdB in our circuit was the wild-type CcdB with a fragment of lacZ $\alpha$  fused to it (see details in reference 37.). The prey could rescue the predator by producing a QS signal (3OC6HSL), which diffused into the predator to induce CcdA expression to inhibit CcdB-mediated killing. The predator produced and excreted another QS signal (3OC12HSL) which crossed the prey cell membrane and elicited CcdB expression, killing the prey.

### Plasmids and cell strains

The plasmids encoding the predator-prey function were detailed previously<sup>37</sup>. The only modification was the introduction of a plasmid Ptet-mCherry into the prey to better differentiate and quantify the predator and the prey populations (the predator cells constitutively expressed GFPuv(lva)). To construct the Ptet-mCherry plasmid, the PCR-amplified mCherry gene was cloned into pProTet.E132 (BD Bioscience Clontech). MG1655 cells were used for both the predator and the prey unless otherwise noted.

### Supplementary Material

Refer to Web version on PubMed Central for supplementary material.

### Acknowledgements

We thank F. Yuan for access to a Kodak fluorescence image station and software (Comsol Multiphysics); F. Arnold and C. Collins for sharing genetic constructs; D. Schaeffer for suggestions on modeling; C. Tan for commenting on the manuscript; and other You lab members for discussions. This study was supported by the National Institutes of Health (5R01CA118486), a David and Lucile Packard Fellowship (L.Y.), a DuPont Young Professor Award (L.Y.), an NIH/NIGMS Biotechnology Predoctoral CBTE Fellowship (to S.P.), and a Duke University Pratt Fellowship for undergraduate research (to M.G.). We thank the anonymous reviewers for critical and constructive suggestions.

### References Cited

1. Falkowski PG, Fenchel T, Delong EF. The microbial engines that drive Earth's biogeochemical cycles. *Science*. 2008; 320:1034–1039. [PubMed: 18497287]
2. Strom SL. Microbial ecology of ocean biogeochemistry: a community perspective. *Science*. 2008; 320:1043–1045. [PubMed: 18497289]
3. Muyzer G, Stams AJ. The ecology and biotechnology of sulphate-reducing bacteria. *Nat Rev Microbiol*. 2008; 6:441–454. [PubMed: 18461075]
4. Jia W, Li H, Zhao L, Nicholson JK. Gut microbiota: a potential new territory for drug targeting. *Nat Rev Drug Discov*. 2008; 7:123–129. [PubMed: 18239669]
5. Dethlefsen L, McFall-Ngai M, Relman DA. An ecological and evolutionary perspective on human-microbe mutualism and disease. *Nature*. 2007; 449:811–818. [PubMed: 17943117]
6. Brenner K, You L, Arnold FH. Engineering microbial consortia: a new frontier in synthetic biology. *Trends Biotechnol*. 2008; 26:483–489. [PubMed: 18675483]
7. Peet R. The measurement of species diversity. *Annual Review of Ecology and Systematics*. 1974; 5:285–307.
8. Jessup CM, et al. Big questions, small worlds: microbial model systems in ecology. *Trends Ecol Evol*. 2004; 19:189–197. [PubMed: 16701253]
9. Loreau M, et al. Biodiversity and ecosystem functioning: current knowledge and future challenges. *Science*. 2001; 294:804–808. [PubMed: 11679658]
10. Ley RE, Peterson DA, Gordon JI. Ecological and evolutionary forces shaping microbial diversity in the human intestine. *Cell*. 2006; 124:837–848. [PubMed: 16497592]

11. Dykhuizen DE. Santa Rosalia revisited: why are there so many species of bacteria? *Antonie Van Leeuwenhoek*. 1998; 73:25–33. [PubMed: 9602276]
12. Staley, JT.; Reysenbach, A-L., editors. *Biodiversity of Microbial Life: Foundation of Earth's Biosphere*. Wiley-Liss; 2001.
13. Ward DM, Ferris MJ, Nold SC, Bateson MM. A natural view of microbial biodiversity within hot spring cyanobacterial mat communities. *Microbiol Mol Biol Rev*. 1998; 62:1353–1370. [PubMed: 9841675]
14. Horner-Devine MC, Carney KM, Bohannon BJ. An ecological perspective on bacterial biodiversity. *Proc Biol Sci*. 2004; 271:113–122. [PubMed: 15058386]
15. Tilman D. The ecological consequences of changes in biodiversity: a search for general principles. *Ecology*. 1999; 80:1455–1474.
16. Chesson P, Kuang JJ. The interaction between predation and competition. *Nature*. 2008; 456:235–238. [PubMed: 19005554]
17. Martin MO. Predatory prokaryotes: an emerging research opportunity. *J Mol Microbiol Biotechnol*. 2002; 4:467–477. [PubMed: 12432957]
18. Jurkevitch E. Predatory behaviors in bacteria - diversity and transitions. *Microbe*. 2007; 2:67–73.
19. Guerrero R, et al. Predatory prokaryotes: predation and primary consumption evolved in bacteria. *Proc Natl Acad Sci U S A*. 1986; 83:2138–2142. [PubMed: 11542073]
20. Esteve I, Gaju N, Mir J, Guerrero R. Comparison of techniques to determine the abundance of predatory bacteria attacking chromatiaceae. *FEMS Microbial Ecology*. 1992; 86:205–211.
21. Lambert C, Morehouse KA, Chang CY, Sockett RE. *Bdellovibrio*: growth and development during the predatory cycle. *Curr Opin Microbiol*. 2006; 9:639–644. [PubMed: 17056298]
22. Shou W, Ram S, Vilar JM. Synthetic cooperation in engineered yeast populations. *Proc Natl Acad Sci U S A*. 2007; 104:1877–1882. [PubMed: 17267602]
23. Hart BA, Zahler SA. Lytic enzyme produced by *Myxococcus xanthus*. *J Bacteriol*. 1966; 92:1632–1637. [PubMed: 5958103]
24. Berleman JE, Chumley T, Cheung P, Kirby JR. Rippling is a predatory behavior in *Myxococcus xanthus*. *J Bacteriol*. 2006; 188:5888–5895. [PubMed: 16885457]
25. Pham VD, Shebelut CW, Diodati ME, Bull CT, Singer M. Mutations affecting predation ability of the soil bacterium *Myxococcus xanthus*. *Microbiology*. 2005; 151:1865–1874. [PubMed: 15941994]
26. Keller L, Surette MG. Communication in bacteria: an ecological and evolutionary perspective. *Nat Rev Microbiol*. 2006; 4:249–258. [PubMed: 16501584]
27. Battin TJ, et al. Microbial landscapes: new paths to biofilm research. *Nat Rev Microbiol*. 2007; 5:76–81. [PubMed: 17170748]
28. Pohnert G, Steinke M, Tollrian R. Chemical cues, defence metabolites and the shaping of pelagic interspecific interactions. *Trends Ecol Evol*. 2007; 22:198–204. [PubMed: 17275948]
29. Dicke M, Sabelis MW. Infochemical terminology: based on cost-benefit analysis rather than origin of compounds? *Functional Ecology*. 1988; 2:131–139.
30. Ianora M, et al. New trends in marine chemical ecology. *Estuaries and Coasts*. 2006; 29:531–551.
31. Waters CM, Bassler BL. Quorum sensing: cell-to-cell communication in bacteria. *Annu Rev Cell Dev Biol*. 2005; 21:319–346. [PubMed: 16212498]
32. Whittaker RH, Feeny PP. Allelochemicals: chemical interactions between species. *Science*. 1971; 171:757–770. [PubMed: 5541160]
33. Weissburg MJ, Ferner MC, Pisut DP, Smee DL. Ecological consequences of chemically mediated prey perception. *J Chem Ecol*. 2002; 28:1953–1970. [PubMed: 12474893]
34. Shiner EK, Rumbaugh KP, Williams SC. Inter-kingdom signaling: deciphering the language of acyl homoserine lactones. *FEMS Microbiol Rev*. 2005; 29:935–947. [PubMed: 16219513]
35. Kerr B, Riley MA, Feldman MW, Bohannon BJ. Local dispersal promotes biodiversity in a real-life game of rock-paper-scissors. *Nature*. 2002; 418:171–174. [PubMed: 12110887]
36. Reichenbach T, Mobilia M, Frey E. Mobility promotes and jeopardizes biodiversity in rock-paper-scissors games. *Nature*. 2007; 448:1046–1049. [PubMed: 17728757]

37. Balagadde FK, et al. A synthetic *Escherichia coli* predator-prey ecosystem. *Mol Syst Biol*. 2008; 4:187. [PubMed: 18414488]
38. Weber W, Daoud-El Baba M, Fussenegger M. Synthetic ecosystems based on airborne inter- and intrakingdom communication. *Proc Natl Acad Sci U S A*. 2007; 104:10435–10440. [PubMed: 17551014]
39. Kosiniski MJ, Rinas U, Bailey JE. Isopropyl- $\beta$ -D-thiogalactopyranoside influences the metabolism of *Escherichia coli*. *Applied Microbiology and Biotechnology*. 1992; 36:782–784.
40. Lauffenburger DA. Quantative studies of bacterial chemotaxis and microbial population dynamics. *Microb Ecol*. 1991; 22:175–185. [PubMed: 24194335]
41. Kelly FX, J DK, Lauffenburger DA. Effect of bacterial chemotaxis on dynamics of microbial competition. *Microb Ecol*. 1988; 16:115–131. [PubMed: 24201566]
42. Woodward DE, et al. Spatio-temporal patterns generated by *Salmonella typhimurium*. *Biophys J*. 1995; 68:2181–2189. [PubMed: 7612862]
43. Keller EF, Segel LA. Traveling bands of chemotactic bacteria: a theoretical analysis. *J Theor Biol*. 1971; 30:235–248. [PubMed: 4926702]
44. Hastings A. Transients: the key to long-term ecological understanding? *Trends Ecol Evol*. 2004; 19:39–45. [PubMed: 16701224]
45. Tilman, D.; Kareiva, P. *Spatial Ecology*. Princeton: Princeton University Press; 1997.
46. Rosenzweig, ML. *Species Diversity in Space and Time*. Cambridge: Cambridge University Press; 1995.
47. Stolp, H. *Microbial Ecology: Organisms, habitats, activities*. Cambridge: Cambridge University Press; 1988.
48. Hastings A. Spatial heterogeneity and the stability of predator-prey systems. *Theor Popul Biol*. 1977; 12:37–48. [PubMed: 918872]
49. Kim HJ, Boedicker JQ, Choi JW, Ismagilov RF. Defined spatial structure stabilizes a synthetic multispecies bacterial community. *Proc Natl Acad Sci U S A*. 2008; 105:18188–18193. [PubMed: 19011107]
50. Brenner K, Karig DK, Weiss R, Arnold FH. Engineered bidirectional communication mediates a consensus in a microbial biofilm consortium. *Proc Natl Acad Sci U S A*. 2007; 104:17300–17304. [PubMed: 17959781]

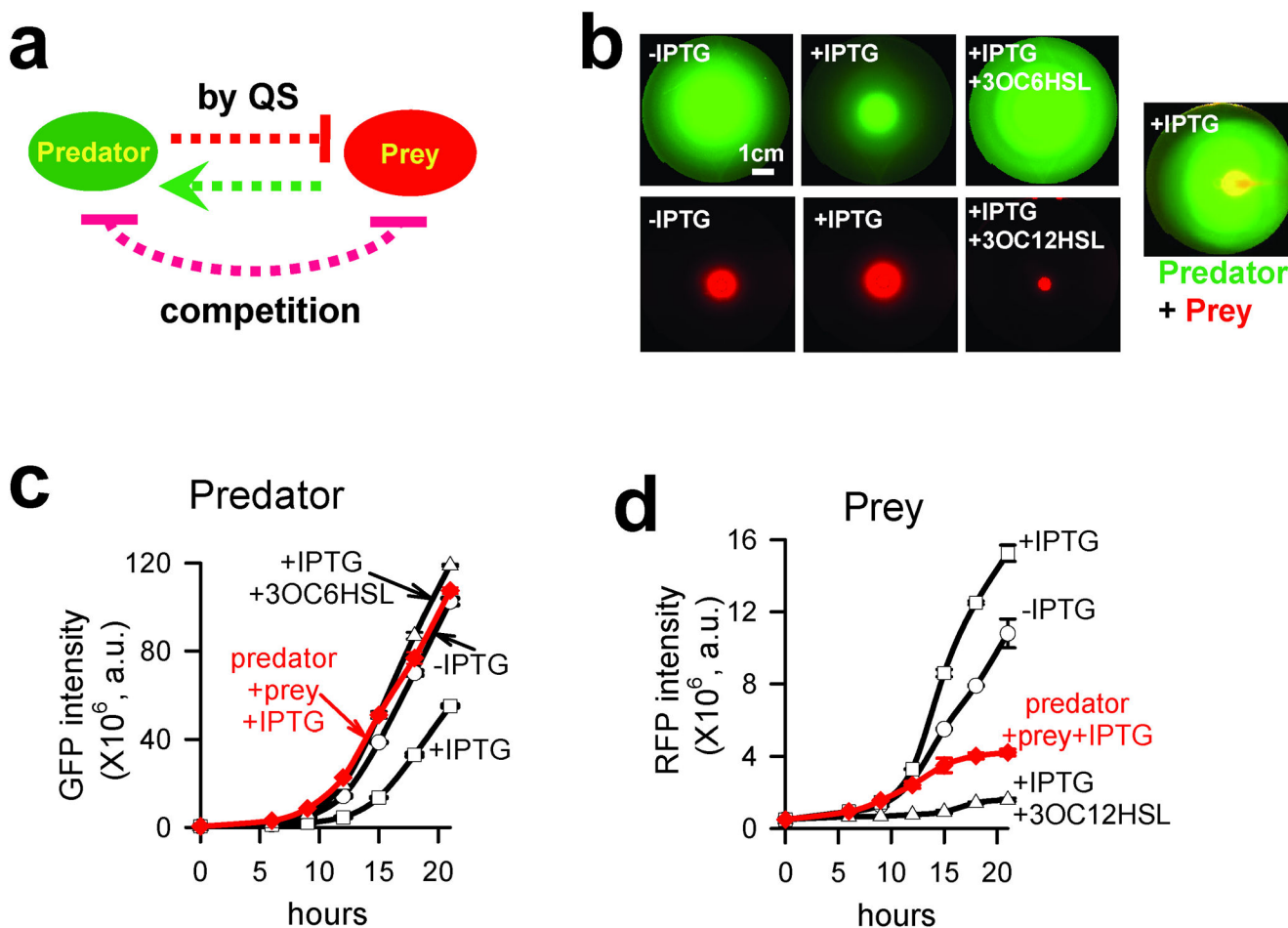


**Figure 1.**

Spatiotemporal dynamics of the predator and the prey in response to IPTG and AHLs in solid phase. The experiments were performed on 0.2% M9 (pH=7) soft agar at 37°C.

(a) The interaction logic of the chemical-mediated synthetic predator-prey ecosystem. The two populations competed for nutrients and followed the programmed predator-prey interaction *via* QS.

(b) A snapshot (at 18<sup>th</sup> hr) of predator (upper panels, green) and prey (bottom panels, red) colonies without IPTG, with IPTG, and with IPTG and the corresponding AHLs. The right panel is a snapshot (at 18<sup>th</sup> hr) of the patterns resulting from the interaction between a predator colony and a prey colony: the plate was seeded with 10 $\mu$ l predator overnight culture ( $\sim 10^6$  cells) and 10 $\mu$ l prey overnight culture ( $\sim 10^6$  cells) 0.5cm apart. The patterns from duplicate measurements were similar; only one was shown.

(c) Predator expansion dynamics without IPTG, with IPTG, with IPTG and 3OC6HSL, and with IPTG and prey. Data for each time point were deduced from images as measured in (b), with the GFP intensity indicating the total predator density in a plate. Each bar indicated the range of GFP intensity measured in duplicate experiments. Unless noted otherwise, IPTG was applied at 1mM and AHLs were applied at 100nM.

(d) Prey expansion dynamics without IPTG, with IPTG, with IPTG and 3OC12HSL, and with IPTG and predator. Data for each time point were deduced from images as measured in

(b), with the RFP intensity indicating the total prey density in a plate. The RFP intensity reported the prey density. Each bar indicated the range of RFP intensity measured in duplicate experiments.

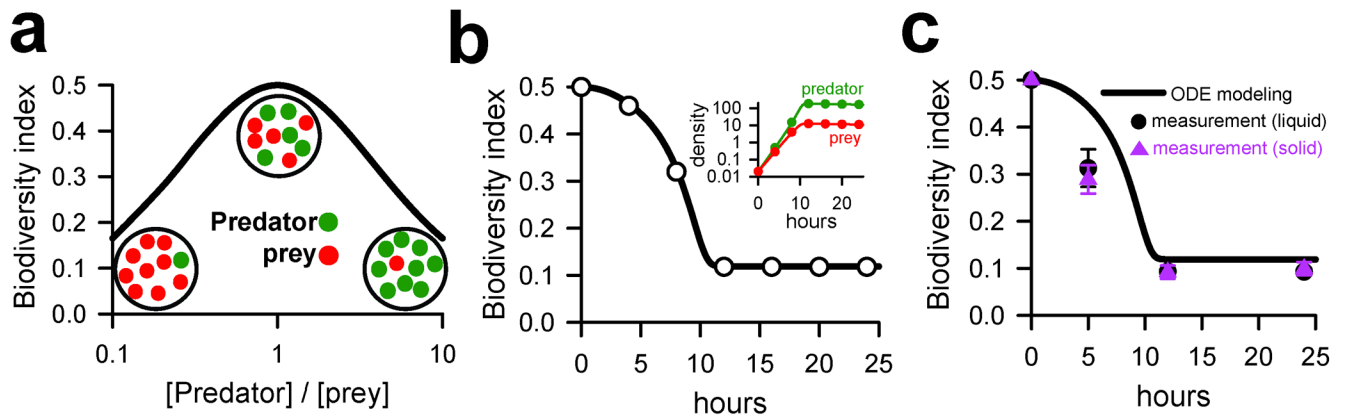


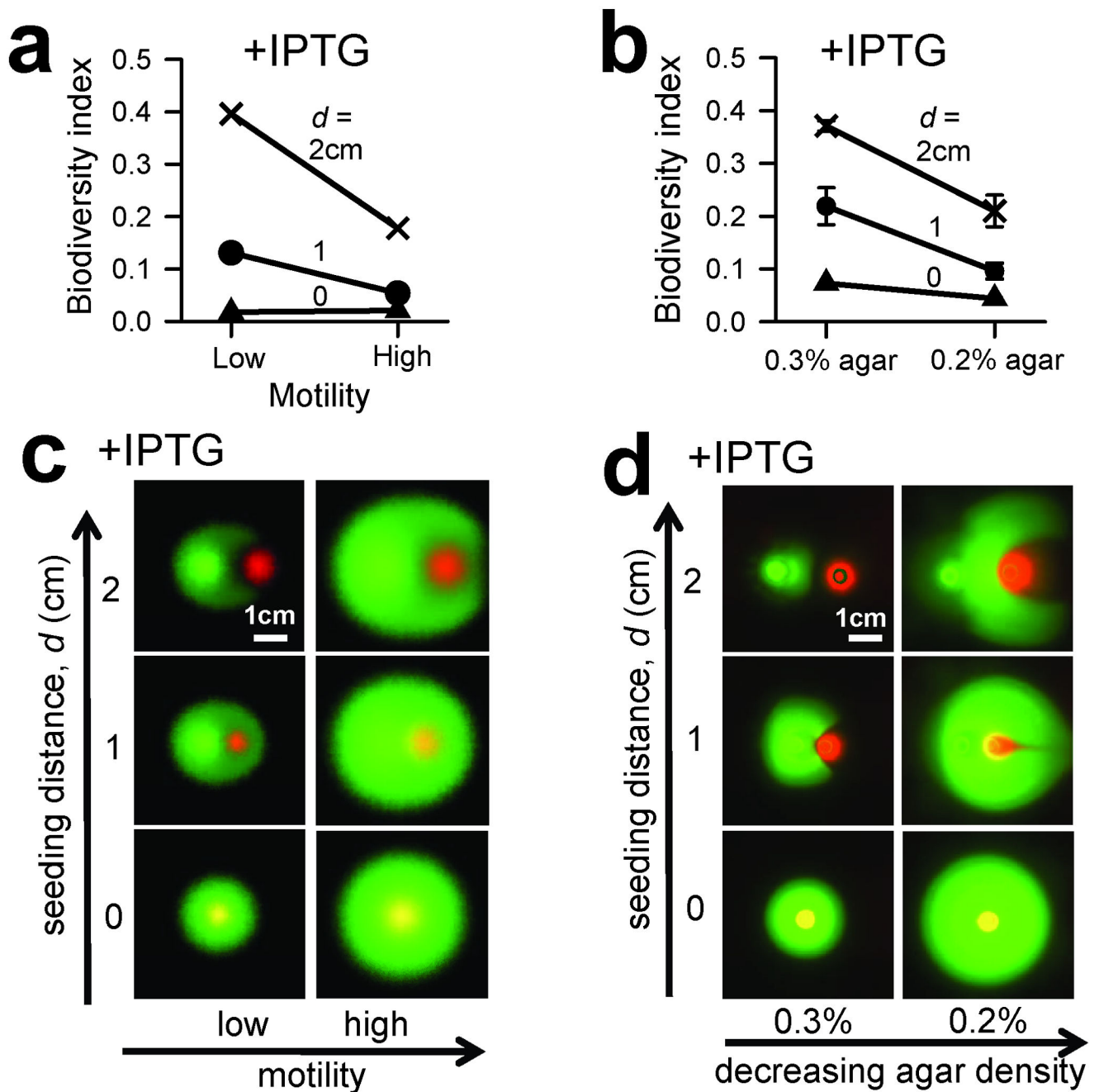
**Figure 2.**

Motility had a minor impact on the biodiversity if the predator and the prey were randomly distributed in close proximity.

(a) Dependence of the BI on the density ratio between the populations.

(b) Simulated time courses of the BI in the liquid (solid line) and solid phases (circles) showed little difference. The inset indicated the time courses of the predator and the prey densities in the liquid phase (solid lines) and the solid phase (dots). At time zero, the same amounts of the predator and the prey cells were seeded in each simulation.

(c) Experimental validation of the simulation results in (b) using fluorescence microscopy measurements. In liquid phase and soft agar (0.4% M9 agar), the biodiversity indices of the ecosystem were essentially identical. Data represented mean values  $\pm$  standard deviation of triplicate experiments at each condition.

**Figure 3.**

Reduced motility promoted biodiversity if seeding habitats were partitioned.

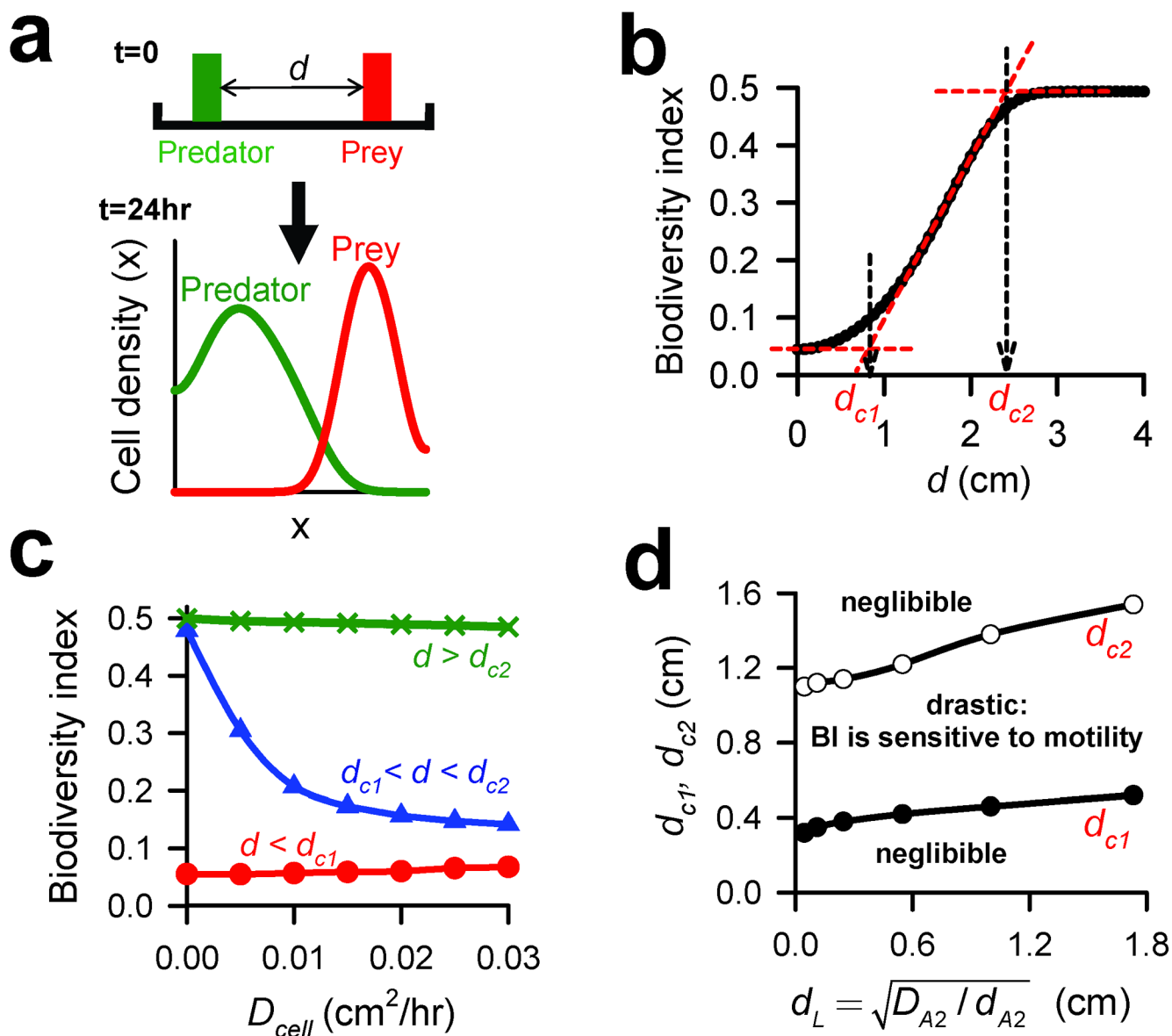
(a) Modeling showed that decreasing motility increased the BI for a sufficient segregation distance ( $d = 1$  or  $2$  cm), but not for  $d = 0$ . To reduce motility in modeling, we decreased the values of the cellular diffusivities ( $D_{p1}$ ,  $D_{p2}$ ) and chemotaxis constants ( $a_1$ ,  $a_2$ ) by four-fold from those of the high motility (base parameter values in Table S1 were used). The BIs were computed based on the predator-prey patterns at 20hr (c).

(b) Experiments validated the model prediction in (a) by using agar density to control motility: 0.2% M9 agar (high motility) and 0.3% M9 agar (low motility). The BIs were

computed based on the snapshots taken at 20hr after seeding the predator and the prey **(d)**. Each error bar indicated the range of the biodiversity index measured in duplicate experiments.

**(c)** Simulated predator-prey patterns at high and low motility with different seeding segregation distances, corresponding to the conditions in **(a)**. Snapshots were taken at 20hr after the simulation initiation.

**(d)** Experimentally measured predator-prey patterns (at 20hr) in 0.2% and 0.3% agar plates with varying seeding segregation distances (0cm, 1cm and 2cm), corresponding to the conditions in **(b)**. The patterns from duplicate experiments were similar; one set was shown.

**Figure 4.**

Two critical segregation distances ( $d_{c1}$ ,  $d_{c2}$ ) in determining the impact of motility on biodiversity.

(a) One-dimensional (1D) distribution of the predator (green) and the prey (red), which were seeded at two focal points with a distance  $d$  (upper panel). The bottom panel showed their density distributions after 24hrs, obtained from numerical simulation of the 1-D PDE model.

(b) The 1-D PDE model revealed two sharp transitions in the dependence of the BI on  $d$ , defining  $d_{c1}$  and  $d_{c2}$ . Below  $d_{c1}$  or above  $d_{c2}$ ,  $d$  had a negligible influence on the BI. For  $d_{c1} < d < d_{c2}$ , the BI increased almost linearly with  $d$ . The spatially averaged BI was calculated at 24hr.

(c) For  $d < d_{c1}$  or  $d > d_{c2}$ , cellular motility had a negligible effect on the BI. For  $d_{c1} < d < d_{c2}$ , the BI decreased almost exponentially with cellular motility.

(d) Both  $d_{c1}$  and  $d_{c2}$  increased with the characteristic length scale of the QS signal diffusion ( $d_L$ ).  $d_L$  was defined by  $\sqrt{D_{A2}/d_{A2}}$ , where  $D_{A2}$  was the diffusivity of 3OC6HSL, and  $d_{A2}$  is the degradation rate of 3OC6HSL. The phase diagram was divided by the “ $d_{c1, 2} \sim d_L$ ” curves into three regions. In the middle region, the cellular motility would drastically influence biodiversity. In the upper and lower regions, cellular motility would have a negligible influence on biodiversity.

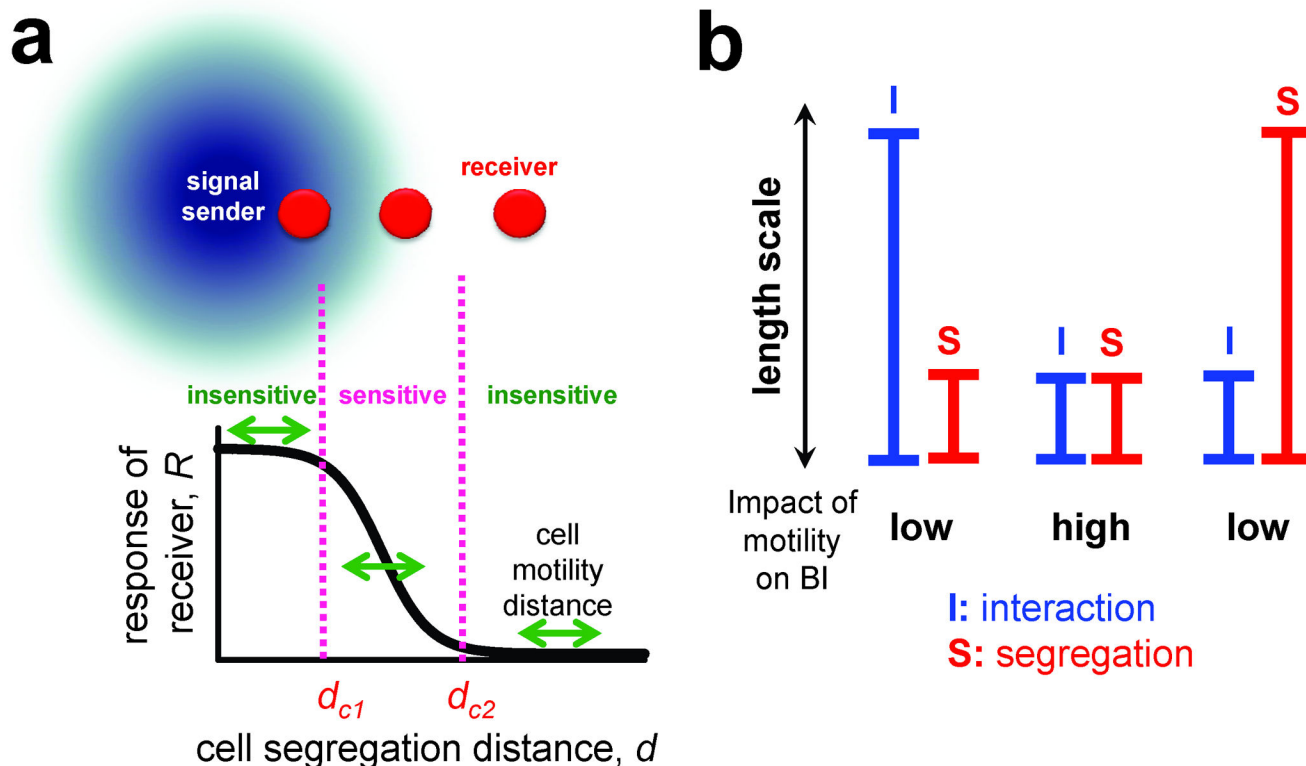


**Figure 5.**

A general criterion in determining the impact of cellular motility on biodiversity.

(a) An abstract model delineated how cellular response ( $R$ ) depends on the cellular segregation distance ( $d$ ) in chemical-mediated ecosystems. The steady-state distribution of a chemical  $A$  satisfied a 1-D PDE:  $D_A \nabla^2 A - d_A A = 0$ , with boundary conditions  $A(0) = A_0$ ,  $A(\infty) = 0$ ; where  $D_A$  was the diffusivity, and  $d_A$  was the degradation rate constant of  $A$ . The analytical solution to this equation was  $A = A_0 e^{-\sqrt{d_A/D_A} x}$ . The response of cells to  $A$  would be  $R = A/(K_A + A)$ , where  $K_A$  was the half maximum response. The double-headed arrow, labeled “cell motility distance,” schematically represented a cell spreading distance (not to scale) by cell motility.

(b) If the interaction length scale was much greater or much smaller than the segregation distance, motility had little impact on biodiversity; if the interaction length scale was comparable to the segregation distance, motility would greatly impact biodiversity.

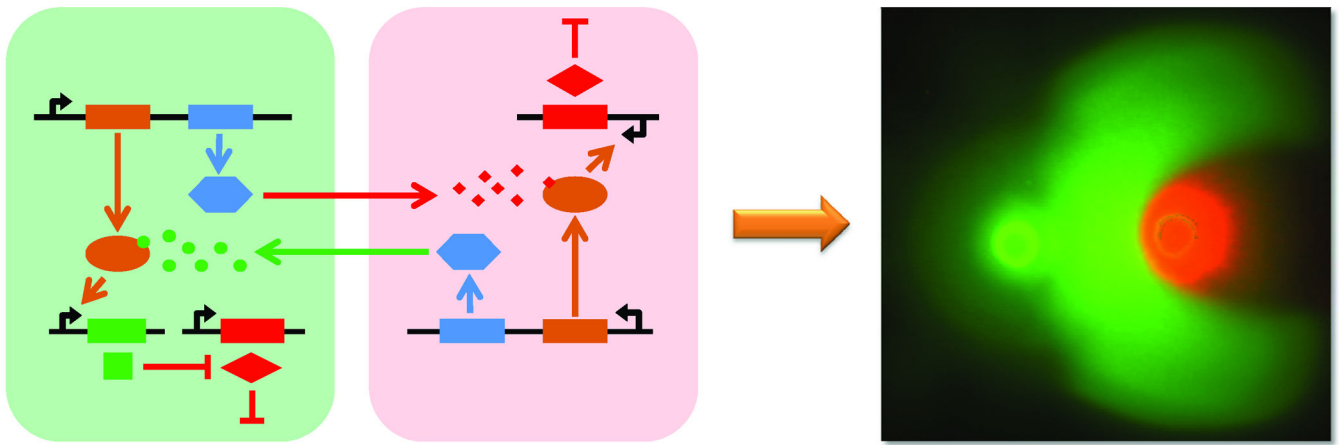


Figure 6.